ACS OMEGA

Open Access

http://pubs.acs.org/journal/acsodf

Article

Correlation Between the Molecular-Level Behavior of Polyurethane on Oily Surfaces and Adhesive Strength

Seito Yamazaki, Takahiro Aizawa, and Takayuki Miyamae*

Cite This: *ACS Omega* 2025, 10, 17468−17475

Read Online

ACCESS | Metrics & More | Article Recommendations | Supporting Information

ABSTRACT: Adhesive bonding is commonly used in various industrial fields. Among the various types of adhesives, polyurethane adhesives have unique properties, such as room-temperature curing, flexibility, and heat insulation, making them indispensable materials in the current automotive and aerospace industries. In these industries, adherends coated with mineral oil or press oil on their surfaces to prevent corrosion are often required, and bonding without degreasing is preferred. Hence, understanding the mechanism of surface adhesion in the presence of oil is crucial. This study aimed to understand the molecular behavior of oil at adherend interfaces and its impact on adhesion. The correlation between the behavior of silicone oil at polyurethane interfaces and adhesion strength was investigated using vibrational sum frequency generation (SFG) spectroscopy, an interface-specific vibrational spectroscopic technique. When polyurethane is cured at room temperature, the silicone oil present at the interface is absorbed into the bulk and disappears from the interface. After being absorbed into the polyurethane during room-temperature curing, the silicone oil remained near the interfacial region, and when the polyurethane was annealed to promote polymerization, it reappeared at the interface, resulting in a significant decrease in adhesion strength. These observations of the behavior of silicone oil at the polyurethane adhesive interface can be explained by the relationships between the solubility of silicone oil, the raw compounds of polyurethane, and polyurethane and provide significant insights into the reliability of adhesion on oily surfaces. They will also contribute to the design of curing behavior for the development of polyurethane adhesives with high adhesion strength to oil-covered adherend surfaces.

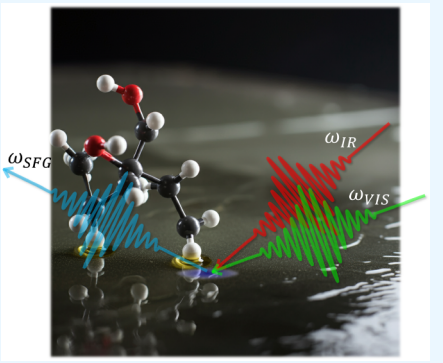

1. INTRODUCTION

Adhesive bonding technology has recently been widely used in a variety of industrial fields to improve fuel efficiency through weight reduction, reduce costs by decreasing person-hours and assembly parts, and diversify bonding materials.[1−8] In particular, in the automobile and aerospace industries, adhesive bonding has attracted much attention as an alternative to mechanical fastening, accompanied by a shift toward using multimaterial components. Among the various adhesives that are used, polyurethane adhesives have unique properties, such as room-temperature curing, flexibility, and thermal insulating properties, making them indispensable materials in myriad industrial fields.[9−11] When joining two components with an adhesive, the condition of the adherend surface significantly affects the bonding characteristics.[12−19] For example, adherend surfaces, such as steel, are often coated with mineral oils to protect against corrosion, and these surfaces should be treated with solvents to ensure adhesion strength and durability.[12] However, this process increases costs and reduces productivity. In addition, solvent usage has many associated drawbacks, such as high environmental impact and health hazards. Therefore, adhesives that can bond and guarantee reliable adhesion strength even when the surface of the adherend is contaminated with oil should be developed. Note that challenges regarding the impact of surface contamination on the reliability and long-term stability of adhesion remain to be resolved. Because a small amount of contamination, such as that encountered when metal is stored under atmospheric conditions, is always present on the surface of the adherend, the resistance to surface contamination in adhesion, the degree of contamination of the adherend surfaces in terms of adhesion strength, and the conditions of the interface are yet to be resolved.[20] This is because the interface between the adhesive and adherend is embedded and, therefore, difficult to examine using analytical techniques. Understanding the mechanism of oil-surface adhesion is crucial to solving these problems, and investigation of the interface between oil-contaminated adherends and adhesives is necessary at the molecular level. Previous studies have primarily used attenuated total internal reflection infrared (ATR-IR) spectroscopy, scanning electron microscopy (SEM), and X-ray photoelectron spectroscopy (XPS) to investigate the interaction between contamination

Received: December 6, 2024
Revised: February 3, 2025
Accepted: April 3, 2025
Published: April 27, 2025

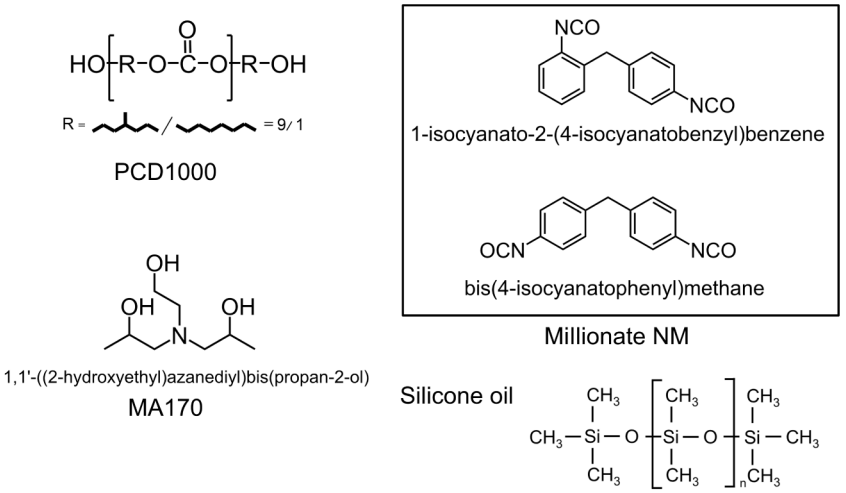

Figure 1. Chemical structures of the materials used in this study.

and adhesives.[21−24] However, because these techniques require sample destruction to expose the adhesive interface, analysis of the interaction and impact of contamination at the embedded interface is limited.

By contrast, sum frequency generation (SFG) spectroscopy is a powerful technique for in situ, nondestructive observation of molecular interactions at surfaces and interfaces.[25] Because SFG uses second-order nonlinear optical effects, information may be obtained regarding the molecular functional groups on surfaces and interfaces, where the inversion symmetry is broken.[26−30] Zhang et al. used SFG and discovered that the formation of urethane bonds at the interface between a polyurethane potting compound and an isocyanate-based primer contributed to an increase in adhesive strength.[28] Xu et al. traced the buried molecular-level structures at the epoxy adhesive/steel interface using SFG and concluded that both hydrogen and chemical bonds play important roles in the formation of the interface and contribute to the interfacial adhesion.[31] Sensui et al. reported the first direct evidence, obtained using SFG, that chemical bonds are formed only at the epoxy polymer surface and the isocyanate primer.[26] In our previous study, the curing behavior of polyurethane at the alumina interfaces was investigated using SFG two-dimensional correlation spectroscopy, with CaF_2 substrates sputtered with thin alumina films as the model substrate of the Al metal surfaces.[20] In addition to the above, SFG spectroscopy is currently widely used for the structural characterization of polymer surfaces and embedded interfaces in adhesives.[32−40]

In this study, SFG spectroscopy was used to investigate the molecular behavior at the interface between a polyurethane adhesive and oil-covered substrates. For this purpose, silicone oil-covered CaF_2 was used as the model system for the oil-contaminated substrate because its SFG spectroscopy has characteristics that can distinguish between the polyurethane-derived SFG peaks and the silicone oil-derived ones.[41] In addition, we conducted a tensile shear test to evaluate the impact on adhesion strength when silicone oil was present on the substrates. Aluminum, a typical lightweight metal used as the main body material for luxury cars, was used as the substrate for the lap-shear test.[42] Furthermore, analysis of the silicone oil present at the polyurethane interfaces at the molecular level was performed using SFG spectroscopy, and CaF_2 substrates sprayed with silicone oil were utilized as the model substrates to investigate the effects of the presence of oil as a contaminant on the surface during the curing reaction of polyurethane. We succeeded in unprecedentedly observing the behavior of silicone oil via SFG by measuring the polyurethane interfaces in the presence of silicone oil, where the adhesive absorbed the silicone oil and resegregated at the interface when cured at high temperatures. The correlation between adhesive strength during polyurethane curing and the presence or absence of silicone oil at the interface provides important insights into the behavior of oil-surface adhesion and the reliability of the adhesion.

2. EXPERIMENTAL SECTION

2.1. Materials. The chemicals used in this study are shown in Figure 1. For the preparation of polyurethane, PCD1000 (Tosoh Corporation, Japan) was used as the polyol, and MA170 (Lion Specialty Chemicals Co. Ltd., Japan) was used as the cross-linking agent. Millionate NM (Tosoh Co., Japan) was used as the isocyanate compound and was used as received. Millionate NM is a mixture of bis(4-isocyanatophenyl)methane and 1-isocyanato-2-(4-isocyanatobenzyl)benzene in a 45:55 molar ratio. Trimethylsilyl-terminated silicone oil (KF-96−50C; Shin-Etsu Chemical Co., Ltd., Japan) was used as received. The molecular weight and degree of polymerization of the silicone oil are 3.5×10^3 g/mol and 4.9×10^3, respectively. Unless otherwise noted, all other reagents were purchased from Fujifilm Wako Chemicals Co. (Japan) and used without further purification. First, Millionate NM (1.84×10^4 mol) and PCD1000 (3.66×10^3 mol) were mixed under a nitrogen atmosphere. This mixture and MA170 (9.86×10^3 mol) were mixed to prepare polyurethane adhesives, then defoamed by vacuum evacuation using a vacuum pump. The ratios are such that the polyol and isocyanate react without an excess or insufficient ratio to form polyurethane.

2.2. Characterization. The SFG system used in this study has been reported previously.[26] In these experiments, a mode-locked Nd:YAG laser (PL2251A−50, Ekspla, Lithuania) with a pulse width of 30 ps and a repetition rate of 50 Hz was used as the master laser source. The sample surface was irradiated with a tunable IR beam and a 532 nm visible beam at incident angles of 45° and 52°, respectively. The SFG spectra were collected in 3 cm^{-1} increments in the CH stretching region

https://doi.org/10.1021/acsomega.4c11036
ACS Omega 2025, 10, 17468−17475

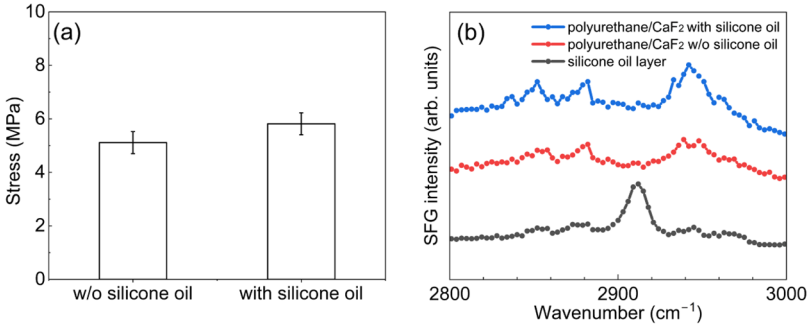

Figure 2. (a) Adhesive strengths of with and without oil-coated Al substrates applied polyurethane. (b) SFG spectra of silicone oil layer on CaF_2 (black) and SFG spectra of polyurethane/CaF_2 substrate interface with (blue) and without silicone oil (red).

(2800 cm^{-1} to 3000 cm^{-1}), and the data were averaged over 300 laser shots. The SFG spectra were collected using the SSP (S-polarized sum frequency, S-polarized visible beam, and P-polarized IR beam) polarization combination.

For the SFG experiments, a 2 mm-thick CaF_2 substrate (30 mmϕ, Pier Optics Co., Ltd., Japan) was ultrasonicated in ethanol and acetone for 15 min each, followed by plasma treatment for 15 min using a plasma cleaner (PDC-32G, Sanyo Trading Co., Ltd., Japan) to remove surface contaminants. Subsequently, a 1 wt % silicone oil hexane solution was sprayed 10 times at a distance of 50 cm from the CaF_2 substrate. The thickness of the sprayed silicone oil was estimated from the change in weight and spraying area and was found to be approximately 100 nm. Immediately after mixing the reagents, the deformed polyurethane was applied to the silicone oil-sprayed CaF_2 substrate and sandwiched with a glass slip (Matsunami Glass Ind., Ltd., Japan). The thickness of the polyurethane was adjusted to 0.89 mm using a spacer. To measure the SFG spectra, laser light was illuminated from the transparent CaF_2 substrate side.

For lap-shear tests, all the Al substrates were polished with a polishing agent and then cleaned with acetone for 30 min to degrease. Then, the samples were prepared by spraying silicone oil diluted with hexane onto the polished aluminum substrates, applying 0.1 mm-thick polyurethane adhesives, and sandwiching them between polished aluminum substrates. We noted that the aluminum surfaces were oxidized, as confirmed by XPS (Figure S1). A tabletop tensile and compression tester (MCT-2150, A&D Company, Ltd., Japan) was used for the lap-shear test. The speed of the tensile test was adjusted to 100 mm/min. Typical load−displacement curves of the Al substrates under various conditions of the cured polyurethanes are shown in Figure S2. In this study, the adhesive strength was estimated by dividing the maximum value of the load−displacement curve by the adhesive area. Therefore, the adhesive strength represents the stress at the sample break. The adhesion strengths were determined by averaging at least seven independent test specimens. The error bars represent the standard deviations for each test specimen.

ATR-IR measurements were performed using an FT/IR-6600 (JASCO Co., Japan). A temperature-controlled thermal control unit (TC-600, JASCO Co., Japan) and an ATR-IR unit (ATRPRO670H−S, JASCO Co., Japan) with a diamond prism were used for measurements during the annealing of polyurethanes up to 150 °C.

3. RESULTS AND DISCUSSION

3.1. Molecular Behavior of Silicone Oil at the Interface. Lap-shear tests were performed on samples with and without silicone oil on the substrate to understand the effect of silicone oil on adhesion after room-temperature curing. The results of the adhesion strength tests for the polyurethane/Al substrates with and without sprayed silicone oil after curing at room temperature are shown in Figure 2a. Contrary to expectations, the adhesion strength of polyurethane cured at room temperature was similar for the samples, regardless of whether silicone oil was sprayed on the Al substrate surfaces. We note that the failure mode of the room-temperature-cured polyurethane was cohesive failure, regardless of silicone oil spraying.

Thereafter, SFG was performed to investigate the molecular behavior of the silicone oil on the polyurethane/CaF_2 substrate after room-temperature curing. First, we identified the peak positions in the SFG analysis of silicone oil to investigate its molecular behavior at the interface between polyurethane and the CaF_2 substrate. The SFG spectrum of the silicone oil layer formed on the CaF_2 substrate alone contains a peak at 2910 cm^{-1} (Figure 2). This peak is attributed to the symmetric stretching vibration of the Si-CH_3 groups in the silicone oil.[43] Because the symmetric Si-CH_3 peak can be observed at a different wavenumber position from that of the stretching vibrations of the methylene (2850 and 2920 cm^{-1}) and methyl (2880, 2940, and 2970 cm^{-1}) groups in the main chain of the polyurethane,[44] the molecular behavior of silicone oil at the polyurethane/CaF_2 interface may be monitored at 2910 cm^{-1}. When polyurethane was applied to CaF_2 substrates coated with silicone oil and cured at room temperature for 20 h, the obtained SFG spectra of the interface were almost identical to those of the samples without silicone oil, despite the silicone oil being spread on the substrate. Furthermore, the peak derived from symmetric Si-CH_3 disappeared.

In general, since the vibrational modes are observed in SFG when the molecules at the interface have net orientation, the disappearance of the SFG signals of functional groups does not simply imply that the molecules are not present at the interface. For example, if the functional groups are in random orientation or horizontal orientation, or if they have a disappearing configuration, then even if the molecules with that functional group are definitely present at the interface, the vibrational modes of SFG cannot be observed.[45,46] Thus, the disappearance of the Si-CH_3 peak is further investigated by changing the amount of silicone oil sprayed onto the CaF_2 substrate and monitoring the behavior of the silicone oil at the interface during room-temperature curing of the polyurethane.

https://doi.org/10.1021/acsomega.4c11036
ACS Omega 2025, 10, 17468−17475

If the orientation of the silicone oil at the interface changes to random orientation due to the curing of the polyurethane, then the Si-CH_3 SFG peak should not be observed regardless of the amount of silicone oil. We note that the amount of silicone oil on the adherend was estimated from the change in weight. The thicknesses of the oil films were estimated by dividing the change in the weight of the adherend by the relative density of the silicone oil to obtain the amount of adhered silicone oil, which was then divided by the total substrate area. This process was repeated five times for each concentration. The film thickness was 55.4 ± 12.9 nm when sprayed with a 1 wt % silicone oil hexane solution and 195 ± 20.6 nm when sprayed with a 5 wt % silicone oil hexane solution. The thickness of the film of silicone oil is considered to be sufficient to interrupt the reaction and interaction between Al, CaF_2, and polyurethane. Figure 3a illustrates the adhesion strength of the room-temperature-cured polyurethane on the Al substrates sprayed with 1 and 5 wt % diluted silicone oil, and the SFG spectra of the polyurethane/CaF_2 substrate interfaces cured at room temperature for 20 h for substrates sprayed with 1 and 5 wt % silicone oil solutions diluted with hexane. As can be observed from the lap-shear tests of the 5 wt % samples, the adhesion strength is clearly lower than that of the samples sprayed with 1 wt % diluted silicone oil. It is interesting to note that the samples sprayed with 1 wt % diluted silicone oil showed cohesive failure, while the samples sprayed with 5 wt % diluted silicone oil showed interface failure. Obviously, for the substrate sprayed with 5 wt % diluted silicone oil, shown in Figure 3, which was cured for 20 h at room temperature, the symmetric stretching vibrations of Si-CH_3 at 2910 cm^{-1} are clearly observed, whereas this peak is not observed for the sample sprayed with 1 wt % silicone oil. This result strongly implies that the disappearance of the peak at 2910 cm^{-1} derived from the 1 wt % sample is not due to the disordering of Si-CH_3. These results suggest that the 1 wt % sprayed silicone oil applied onto CaF_2 was absorbed into the bulk of the polyurethane during room-temperature curing and disappeared from the CaF_2 interface. This type of absorption of silicone oils into adhesives has also been reported in the case of epoxy adhesives.[29] The results of the lap-shear strength tests also suggest that 1 wt % sprayed silicone oil has no impact on the shear strength of the interfaces, even in room-temperature-cured polyurethane, thereby indirectly indicating that the silicone oil is absorbed into the bulk of the polyurethane.

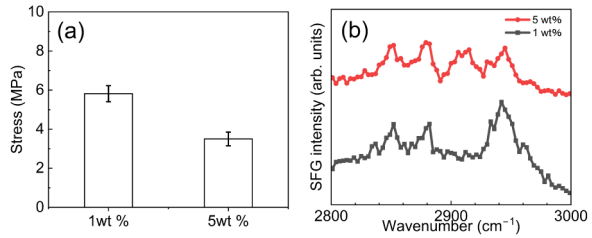

Figure 3. (a) Adhesive strengths of polyurethane samples cured at room temperature for 20 h on Al substrates sprayed with 1 and 5 wt % silicone oil diluted solutions. (b) SFG spectra of the polyurethane/CaF_2 substrate interfaces when sprayed with 1 wt % (black) and 5 wt % (red) silicone oils and cured at room temperature.

The absorption of silicone oil into polyurethane can be explained in terms of the solubility parameters of silicone oil, polyols, and isocyanates. The solubility parameters of PCD1000, MA170, and MDI, obtained by the group contribution method, are 22.0 $(J/cm^3)^{1/2}$, 29.4 $(J/cm^3)^{1/2}$, and 25.7 $(J/cm^3)^{1/2}$, respectively,[47,48] while the solubility parameter of silicone oil is 15.6 $(J/cm^3)^{1/2}$.[49] In contrast, the solubility parameter of polyurethane is 37.2 $(J/cm^3)^{1/2}$ which is very different from that of silicone oil.[49] Hence, immediately after the polyurethane is applied to the CaF_2 substrates, silicone oil and the raw compounds of polyurethane are partially dissolved into each other because both are in a liquid state. If the polymerization reaction progresses, the solubility of silicone oil into polyurethane will decrease due to the difference in solubility parameters. However, as shown in the ATR-IR spectra in Figure S3a, a considerable number of unreacted NCO and OH groups remain in the bulk even after 20 h of room-temperature curing. Consequently, we concluded that silicone oil remains in the bulk even after 20 h of room-temperature curing.

Furthermore, the above hypothesis suggests that silicone oil has poor solubility with room-temperature-cured polyurethane. The fact that the polyurethane cannot absorb all of the silicone oil suggests that the absorbed silicone oil remains near the polyurethane interfacial region. We will refer to this hypothesis again later . Moreover, because the SFG spectral shapes of the polyurethane shown in Figure 3 are similar—excluding that of the Si-CH_3 peak located at 2910 cm^{-1} regardless of the amount of silicone oil, we conclude that the presence of silicone oil does not significantly affect the curing reaction of polyurethane at room temperature at the interface.

3.2. Impact of Postannealing After Room-Temperature Curing. Polyurethane is produced by the polymerization reaction of isocyanates and polyols, as shown in Scheme 1. As shown in Figure S3b, the adhesion strength of polyurethane becomes obviously higher when it is further annealed than when it is cured at room temperature for 20 h. This is because the peak derived from the NCO stretching vibration of isocyanate is still observed at 2270 cm^{-1} after 20 h of room-temperature curing, as shown in Figure S3a, and hence the cross-linking reaction is incomplete.[50] By applying further annealing for 20 min at 150 °C, the NCO stretching vibration at 2270 cm^{-1} disappears completely, indicating that polyurethane polymerization is complete.

Scheme 1. Polymerization Reaction of Polyurethane

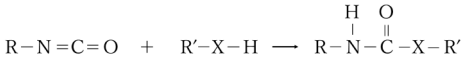

Lap-shear tests and SFG measurements were performed on samples annealed for 20 min at 180 °C after room-temperature curing to investigate how annealing affected the conditions of the adhesive interface. The lap-shear tests (Figure 4 a) indicated that the adhesion strength of the Al substrates sprayed with 1 wt % diluted silicone oil, which were further annealed after room-temperature curing, tended to be lower than that of the samples cured only at room temperature. Furthermore, the interface failure mode changed from cohesive failure to interface failure due to the postannealing of Al substrates sprayed with 1 wt % diluted silicone oil. The SFG spectra of the polyurethane/CaF_2 interfaces cured for 20 h at room temperature and further annealed at 180 °C for 20 min are shown in Figure 4. The SFG spectra of the annealed samples contained an SFG peak derived from Si-CH_3, which was not observed in the samples cured at room temperature.

https://doi.org/10.1021/acsomega.4c11036
ACS Omega 2025, 10, 17468−17475

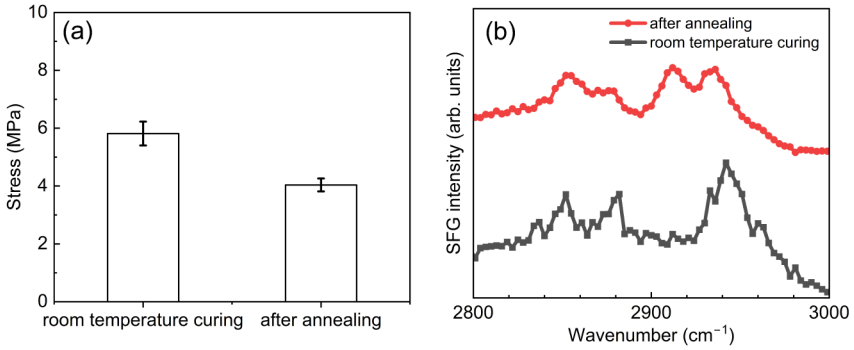

Figure 4. (a) Adhesive strengths of polyurethane applied to oil-coated Al substrates after curing at room temperature and after annealing at 180 °C for 20 min. (b) SFG spectra at the polyurethane/CaF_2 substrate interface after room-temperature curing (black) and after annealing at 180 °C for 20 min (red).

Hence, the silicone oil absorbed into the polyurethane during room-temperature curing segregates again at the interface during thermal annealing. Additionally, it is highly likely that the adhesion strength is reduced because of the segregation of silicone oil caused by thermal annealing.

Resegregation of silicone oil at the polyurethane/CaF_2 interfaces can also be explained in terms of the solubility parameters of silicone oil and polyurethane. As previously mentioned, the solubility parameter of silicone oil is 15.6 $(J/cm^3)^{1/2}$, whereas the solubility parameter of cured polyurethane is 37.2 $(J/cm^3)^{1/2}$.[49] Thus, as the polymerization reaction progresses through annealing, the affinity between polyurethane and silicone oil gradually decreases. As a result, silicone oil separates at the interface. Thus, we conclude that this resegregation behavior strongly suggests that the silicone oil absorbed into the polyurethane during room-temperature curing remains near the interface due to the difference in solubility parameters between polyurethane and silicone oil. Additionally, the segregation of silicone oil owing to thermal annealing can be attributed to the segregation of low-molecular-weight components. Polyurethane becomes a robust solid as the molecular weight increases, while the polymerization reaction proceeds during annealing. The molecular weight of silicone oil used in this study is smaller than that of fully cured polyurethane. Since silicone oil does not participate in the polymerization reaction, as described in the preceding section, it segregated at the interface as the polymerization reaction of polyurethane progressed with annealing. The segregation of low-molecular-weight dPS to the surface in a mixture of polystyrene (PS) and deuterated polystyrene (dPS) was also confirmed via static secondary ion mass spectrometry and neutron reflectometry.[51] Segregation of low-molecular-weight components at the interface that is caused by thermal annealing has been previously reported for polypropylene mixed with a small amount of maleic anhydride-modified polypropylene.[27]

3.3. Impact of the Annealing Process on the Interface Segregation of Silicone Oil. Next, we investigated the effect of the annealing procedure on the segregation behavior of silicone oil. One method involves curing at room temperature, followed by stepwise annealing and then annealing at 150 °C for 20 min (Figure 5 a). Second, the samples were rapidly annealed after room-temperature curing and maintained at 150 °C for 20 min (Figure 5). As the total amount of thermal energy applied to the samples differed between the two annealing procedures, the polymerization reactions in the

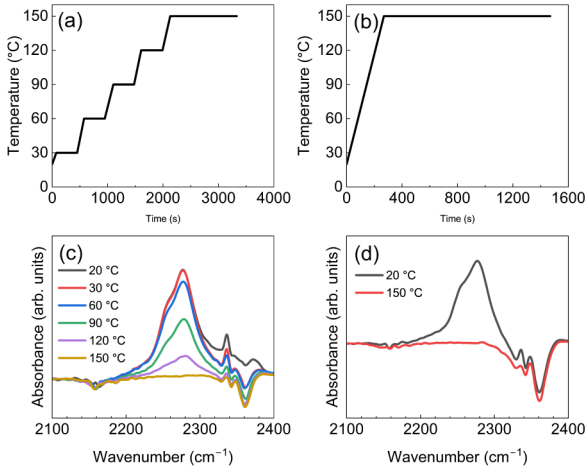

Figure 5. Schematic diagrams of (a) sequential annealing and (b) rapid annealing processes. ATR-IR spectra in NCO stretching vibration region of polyurethane during room-temperature curing after (c) sequential annealing and (d) rapid annealing processes.

polyurethanes were confirmed via ATR-IR in the NCO stretching region for each annealing condition. As shown in Figure 5 c and d, for both annealing procedures, the 2270 cm^{-1} peak derived from the NCO stretching vibration of isocyanate disappears completely after annealing at 150 °C for 20 min, indicating that the polymerization is complete. The results of the lap-shear tests (Figure 6) indicate that the adhesion

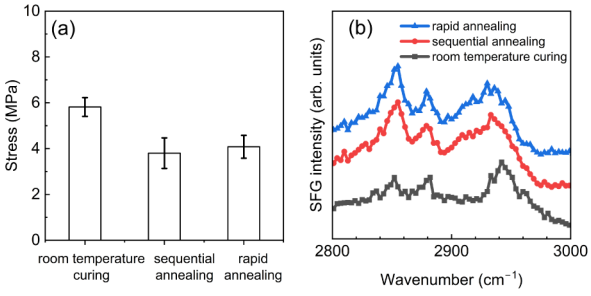

Figure 6. (a) Adhesive strengths of polyurethane applied to oil-coated Al after room-temperature curing, sequential, and rapid annealing. (b) SFG spectra acquired from the polyurethane/oil-coated CaF_2 substrate interfaces after room-temperature curing (black), SFG spectra of the polyurethane/oil-coated CaF_2 substrate interface after sequential (red), and rapid (blue) annealing.

https://doi.org/10.1021/acsomega.4c11036
ACS Omega 2025, 10, 17468−17475

strength decreased for the samples that had undergone annealing, compared with that of the specimens that were cured at room temperature only, because of the segregation of silicone oil at the interface, as described in the preceding section. However, no significant difference was observed in the adhesion strength of polyurethane for the samples that underwent these thermal treatment procedures.

This phenomenon is further confirmed by the SFG spectra acquired from the polyurethane/1 wt % silicone oil-sprayed CaF_2 interfaces (Figure 6b) for the two annealing methods. For comparison, the SFG spectra of the polyurethane interface cured at room temperature are also shown. In the SFG spectra of both annealed samples, the Si-CH_3 peak derived from the silicone oil appears as a shoulder at 2910 cm^{-1}, and no significant difference exists between these spectra. Therefore, in both heating procedures, silicone oil was segregated at the interface by annealing.

4. CONCLUSION

The behavior of silicone oil at the adhesive interface of polyurethane on oily surfaces was investigated. Despite the use of different substrates in the SFG and lap-shear tests, a good correlation was observed between the SFG and lap-shear test results, which confirmed that the presence of silicone oil at the interface significantly reduced the adhesion strength. Silicone oil was absorbed into the polyurethane when cured at room temperature and had no impact on the adhesion strength. By contrast, when the polyurethane was annealed to complete the polymerization reaction, the adhesion strength decreased notably. This is consistent with the SFG results, which indicate that the silicone oil segregated again at the interface owing to the progress of the polymerization reaction caused by annealing. These phenomena can be explained in terms of the solubility between polyurethane and silicone oil. The solubility parameter values of polyurethane raw materials and silicone oil are relatively closer than those of polyurethane itself, and silicone oil is absorbed into the polyurethane bulk at the initial stage of room-temperature curing. On the other hand, as the curing reaction proceeds due to postannealing, silicone oil becomes less soluble in polyurethane and segregates again at the interface. This suggests that silicone oil, once absorbed into polyurethane, remains close to the interfacial region.

This study highlights the effectiveness of SFG as a valuable technique for nondestructive inspection of tiny amounts of contamination at buried solid−solid interfaces. SFG analysis revealed a unique phenomenon in which polyurethane absorbs a tiny amount of silicone oil adhered to the adherend during room-temperature curing and maintains adhesion strength nearly equal to that of clean surfaces. In contrast, the absorbed oil in the polyurethane resegregates at the interface during annealing, resulting in reduced adhesion strength. The above suggests that controlling the solubility between the adhesive and the oil is an important factor, even in oily surface adhesion. Understanding the migration behavior of silicone oil at the polyurethane adhesive interface is extremely useful in constructing practical adhesive interfaces, and these insights are critical for understanding the impact of adhesive/oil-covered adherend interfaces on adhesion properties, such as delamination and durability. It will also be useful for the development of polyurethane adhesives with higher adhesion strength to oil-covered adherend surfaces by designing their curing behaviors.

ASSOCIATED CONTENT

Supporting Information

The Supporting Information is available free of charge at https://pubs.acs.org/doi/10.1021/acsomega.4c11036.

XPS spectra for the polished Al substrate for the lap-share tests, Typical load−displacement curves for each lap-share test, ATR-IR spectra in the NCO region of polyurethane before curing, after room-temperature curing for 20 h, and postannealing at 150 °C for 20 min after room-temperature curing, adhesive strengths of polyurethane applied to Al substrates after curing at room temperature and after annealing at 150 °C for 20 min (PDF)

AUTHOR INFORMATION

Corresponding Author

Takayuki Miyamae − *Graduate School of Science and Engineering, Chiba University, Chiba 263-8522, Japan; Molecular Chirality Research Center, Chiba-shi 263-8522, Japan; Soft Molecular Activation Research Center, Chiba 263-8522, Japan;* orcid.org/0000-0001-6543-5820; Email: t-miyamae@chiba-u.jp

Authors

Seito Yamazaki − *Graduate School of Science and Engineering, Chiba University, Chiba 263-8522, Japan*

Takahiro Aizawa − *Polyurethane Research Laboratory, Tosoh Co., Yokkaichi, Mie 510-8540, Japan*

Complete contact information is available at: https://pubs.acs.org/10.1021/acsomega.4c11036

Author Contributions

S.Y. and T.M.: conceptualization; S.Y. and T.A.: sample preparation; S.Y.: data curation; S.Y., T.A., and T.M.: investigation and writing—original draft preparation; T.M.: supervision and project administration.

Notes

The authors declare no competing financial interest.

ACKNOWLEDGMENTS

This work was partly supported by JSPS KAKENHI Grants-in-Aid for Scientific Research (22H02048 and 23K17811), Japan, and Tosoh Co.

REFERENCES

(1) Malekinejad, H.; Carbas, R. J.; Akhavan-Safar, A.; Marques, E. A.; Castro Sousa, F.; da Silva, L. F. Enhancing fatigue life and strength of adhesively bonded composite joints: A comprehensive review. *Materials* **2023**, *16*, 6468.

(2) Budzik, M. K.; Wolfahrt, M.; Reis, P.; Kozłowski, M.; Sena-Cruz, J.; Papadakis, L.; Saleh, M. N.; Machalicka, K. V.; Teixeira de Freitas, S.; Vassilopoulos, A. P. Testing mechanical performance of adhesively bonded composite joints in engineering applications: An overview. *J. Adhes.* **2021**, *98*, 2133−2209.

(3) Berntsen, J. F.; Morin, D.; Clausen, A. H.; Langseth, M. Experimental investigation and numerical modelling of the mechanical response of a semi-structural polyurethane adhesive. *Int. J. Adhes. Adhes.* **2019**, *95*, 102395.

(4) Bartczak, B.; Mucha, J.; Trzepieciński, T. Stress distribution in adhesively-bonded joints and the loading capacity of hybrid joints of car body steels for the automotive industry *Int. J. Adhes. Adhes.* **2013**, *45*, 42−52.

(5) Apalak, Z. G.; Apalak, M. K.; Davies, R. Analysis and design of adhesively bonded tee joints with a single support plus angled reinforcement. *J. Adhes. Sci. Technol.* **1996**, *10*, 681−724.
(6) Banea, M. D.; Rosioara, M.; Carbas, R. J. C.; Da Silva, L. F. M. Multi-material adhesive joints for automotive industry. *Composites, Part B* **2018**, *151*, 71−77.
(7) Budhe, S.; Banea, M. D.; de Barros, S.; Da Silva, L. F. M. An updated review of adhesively bonded joints in composite materials. *Int. J. Adhes. Adhes.* **2017**, *72*, 30−42.
(8) He, X. A review of finite element analysis of adhesively bonded joints. *Int. J. Adhes. Adhes.* **2011**, *31*, 248−264.
(9) Das, A.; Mahanwar, P. A brief discussion on advances in polyurethane applications. *Adv. Ind. Eng. Polym. Res.* **2020**, *3*, 93−101.
(10) Banea, M. D.; da Silva, L. F. M.; Campilho, R. D. The Effect of Adhesive Thickness on the Mechanical Behavior of a Structural Polyurethane Adhesive. *J. Adhes.* **2015**, *91*, 331−346.
(11) Boutar, Y.; Naïmi, S.; Mezlini, S.; da Silva, L. F.; Ali, M. B. S. Characterization of aluminium one-component polyurethane adhesive joints as a function of bond thickness for the automotive industry: Fracture analysis and behavior. *Eng. Fract. Mech.* **2017**, *177*, 45−60.
(12) Baldan, A. Adhesively-bonded joints and repairs in metallic alloys, polymers and composite materials: Adhesives, adhesion theories and surface pretreatment. *J. Mater. Sci.* **2004**, *39*, 1−49.
(13) Marques, A. C.; Mocanu, A.; Tomić, N. Z.; Balos, S.; Stammen, E.; Lundevall, A.; Abrahami, S. T.; Günther, R.; de Kok, J. M. M.; Teixeira de Freitas, S. Review on Adhesives and Surface Treatments for Structural Applications: Recent Developments on Sustainability and Implementation for Metal and Composite Substrates. *Materials* **2020**, *13*, 5590.
(14) Reis, P. N. B.; Ferreira, J. M.; Richardson, M. O. W. Effect of the Surface Preparation on PP Reinforced Glass Fiber Adhesive Lap Joints Strength. *J. Thermoplast. Compos. Mater.* **2012**, *25*, 3−13.
(15) Tornow, C.; Schlag, M.; Lima, L. C. M.; Stübing, D.; Hoffmann, M.; Noeske, P. L. M.; Brune, K.; Dieckhoff, S. Quality assurance concepts for adhesive bonding of composite aircraft structures−characterisation of adherent surfaces by extended NDT. *J. Adhes. Sci. Technol.* **2015**, *29*, 2281−2294.
(16) Akiyama, H.; Fukata, T.; Sato, T.; Horiuchi, S.; Sato, C. Influence of surface contaminants on the adhesion strength of structural adhesives with aluminium. *J. Adhes.* **2020**, *96*, 1311−1325.
(17) Leena, K. K. K. A.; Athira, K. K.; Bhuvaneswari, S.; Suraj, S.; Rao, V. L. Effect of surface pre-treatment on surface characteristics and adhesive bond strength of aluminium alloy. *Int. J. Adhes. Adhes.* **2016**, *70*, 265−270.
(18) Crook, R. A.; Sinclair, J. W.; Poulter, L. W.; Schulte, K. J. An environmentally-friendly process for bonding aluminum using aqueous metasilicate sol-gel and silane adhesion promoters. *J. Adhes.* **1998**, *68*, 315−329.
(19) Fuyama, N.; Okada, K.; Nagaoka, T.; Nishimoto, A. Improvement of Surface Properties of Aluminum Alloy-Based Composites by Multi-Layer DLC Coating. *Mater. Trans.* **2022**, *63*, 1462−1468.
(20) Horiuchi, S.; Terasaki, N.; Miyamae, T. *Interfacial Phenomena in Adhesion and Adhesive Bonding*; Springer Nature: Singapore, 2023.
(21) Greiveldinger, M.; Shanahan, M. E.; Jacquet, D.; Verchère, D. Oil-covered substrates: A model study of the evolution in the interphase during cure of an epoxy adhesive. *J. Adhes.* **2000**, *73*, 179−195.
(22) Jeenjitkaew, C.; Luklinska, Z.; Guild, F. Morphology and surface chemistry of kissing bonds in adhesive joints produced by surface contamination. *Int. J. Adhes. Adhes.* **2010**, *30*, 643−653.
(23) Brandão, R.; Borges, C.S.P.; Marques, E.A.S.; Carbas, R.J.C.; Akhavan-Safar, A.; Nunes, P.D.P.; Ueffing, C.; Weißgraeber, P.; Schmid, F.; da Silva, L.F.M. Effect of surfactant contamination on the properties of aluminum/silicone adhesive joints. *Mech. Adv. Mater. Struct.* **2022**, *30*, 1875−1888.
(24) Rider, A. N.; Olsson-Jacques, C. L.; Arnott, D. R. Influence of adherend surface preparation on bond durability. *Surf. Interface Anal.* **1999**, *27*, 1055−1063.
(25) Shen, Y. R. Surface properties probed by second-harmonic and sum-frequency generation. *Nature* **1989**, *337*, 519−525.
(26) Sensui, K.; Tarui, T.; Miyamae, T.; Sato, C. Evidence of chemical-bond formation at the interface between an epoxy polymer and an isocyanate primer. *Chem. Commun.* **2019**, *55*, 14833−14836.
(27) Liu, Y.; Shigemoto, Y.; Hanada, T.; Miyamae, T.; Kawasaki, K.; Horiuchi, S. Role of chemical functionality in the adhesion of aluminum and isotactic polypropylene. *ACS Appl. Mater. Interfaces.* **2021**, *13*, 11497−11506.
(28) Zhang, S.; Andre, J. S.; Hsu, L.; Toolis, A.; Esarey, S. L.; Li, B.; Chen, Z. Nondestructive in situ detection of chemical reactions at the buried interface between polyurethane and isocyanate-based primer. *Macromolecules* **2022**, *53*, 10189−10197.
(29) Akaike, K.; Akiyama, H. Direct observation of oil-surface adhesion via sum frequency generation spectroscopy. *J. Adhes.* **2023**, *99*, 1933−1946.
(30) Miyamae, T.; Akiyama, H.; Yoshida, M.; Tamaoki, N. Characterization of poly (N-isopropylacrylamide)-grafted interfaces with sum-frequency generation spectroscopy. *Macromolecules* **2007**, *40*, 4601−4606.
(31) Xu, Z.; Zhang, Y.; Wu, Y.; Lu, X. Spectroscopically Detecting Molecular-Level Bonding Formation between an Epoxy Formula and Steel. *Langmuir* **2022**, *38*, 13261−13271.
(32) Roy, S.; Freiberg, S.; Leblanc, C.; Hore, D. K. Surface structure of acrylate polymer adhesives. *Langmuir* **2017**, *33*, 1763−1768.
(33) Zhang, S.; Hsu, L.; Toolis, A.; Li, B.; Zhou, J.; Lin, T.; Chen, Z. Investigation of the atmospheric moisture effect on the molecular behavior of an isocyanate-based primer surface. *Langmuir* **2021**, *37*, 12705−12713.
(34) Zhang, C.; Hankett, J.; Chen, Z. Molecular level understanding of adhesion mechanisms at the epoxy/polymer interfaces. *ACS Appl. Mater. Interfaces.* **2012**, *4*, 3730−3737.
(35) Akaike, K.; Shimoi, Y.; Miura, T.; Morita, H.; Akiyama, H.; Horiuchi, S. Disentangling origins of adhesive bonding at interfaces between epoxy/amine adhesive and aluminum. *Langmuir* **2023**, *39*, 10625−10637.
(36) Zhang, S.; Zhang, J.; Ding, C.; Ling, Q.; Yuan, Q.; Gan, W. Revealing Interfacial Structures between Silica and Epoxy Adhesive via Spectroscopy and Morphological and Adhesion Tests. *J. Phys. Chem. C* **2024**, *128*, 3857−3867.
(37) Wu, Y.; Lin, T.; Santos, E.; Ahn, D.; Marson, R.; Sarker, P.; Chen, X.; Gubbels, F.; Shephard, N.; Mohler, C.; Wei, T.; Kuo, T.; Chen, Z. Molecular behavior of silicone adhesive at buried polymer interface studied by molecular dynamics simulation and sum frequency generation vibrational spectroscopy. *Soft Matter* **2024**, *20*, 4765−4775.
(38) Lin, T.; Wu, Y.; Santos, E.; Chen, X.; Gubbels, F.; Shephard, N.; Mohler, C.; Ahn, D.; Kuo, T.; Chen, Z. Elucidating the Changes in Molecular Structure at the Buried Interface of RTV Silicone Elastomers during Curing. *Langmuir* **2024**, *40*, 5968−5977.
(39) Wu, Y.; Wang, T.; Fay, J. D.; Zhang, L.; Hirth, S.; Hankett, J.; Chen, Z. Silane Effects on Adhesion Enhancement of 2K Polyurethane Adhesives. *Langmuir* **2023**, *39*, 19016−19026.
(40) Chen, X.; Rossi, D.; Guo, Y.; Wan, Q. G.; Chen, X.; Mohler, C. E.; Kuo, T.; Chen, Z. Effect of Corona Treatment on the Adhesion between a Two-Component Polyurethane Adhesive and Polypropylene. *Macromolecules* **2024**, *57*, 6646−6656.
(41) Kim, C.; Gurau, M. C.; Cremer, P. S.; Yu, H. Chain Conformation of Poly(dimethyl siloxane) at the Air/Water Interface by Sum Frequency Generation. *Langmuir* **2008**, *24*, 10155−10160.
(42) Cavezza, F.; Boehm, M.; Terryn, H.; Hauffman, T. A Review on Adhesively Bonded Aluminium Joints in the Automotive Industry. *Metals* **2020**, *10*, 730.
(43) Lin, T.; Wu, Y.; Santos, E.; Chen, X.; Ahn, D.; Mohler, C.; Chen, Z. Molecular Insights into Adhesion at a Buried Silica-Filled Silicone/Polyethylene Terephthalate Interface. *Langmuir* **2020**, *36*, 15128−15140.

https://doi.org/10.1021/acsomega.4c11036
ACS Omega 2025, 10, 17468−17475

(44) Clarke, M. L.; Wang, J.; Chen, Z. Sum frequency generation studies on the surface structures of plasticized and unplasticized polyurethane in air and in water. *Anal. Chem.* **2003**, *75*, 3275−3280.
(45) Ji, N.; Ostroverkhov, V.; Lagugné-Labarthet, F.; Shen, Y. -R. Surface vibrational spectroscopy on shear-aligned poly-(tetrafluoroethylene) films. *J. Am. Chem. Soc.* **2003**, *125* (47), 14218−14219.
(46) Liu, W.; Zhang, L.; Shen, Y. R. *Chem. Phys. Lett.* **2005**, *412*, 206−209.
(47) Yamamoto, T.; Furukawa, H. Prediction of Mechanical Properties of Glassy Polymers by Group Contribution Method. *Koubunshi Ronbunshu* **1995**, *52*, 187−193.
(48) Fedors, R. F. A method for Estimating Both the Solubility Parameters and Molar Volumes of Liquids. *Polym. Eng. Sci.* **1974**, *14*, 147−154.
(49) Yilgör, I.; Yilgör, E.; Wilkes, G. L. Critical parameters in designing segmented polyurethanes and their effect on morphology and properties: A comprehensive review. *Polymer* **2015**, *58*, A1−A36.
(50) Attaei, M.; Loureiro, M. V.; Do Vale, M.; Condeço, J. A.; Pinho, I.; Bordado, J. C.; Marques, A. C. Isophorone diisocyanate (IPDI) microencapsulation for mono-component adhesives: Effect of the active H and NCO sources. *Polymers* **2018**, *10*, 825.
(51) Tanaka, K.; Kajiyama, T.; Takahara, A.; Tasaki, S. A novel method to examine surface composition in mixtures of chemically identical two polymers with different molecular weights. *Macromolecules* **2002**, *35*, 4702−4706.

https://doi.org/10.1021/acsomega.4c11036
ACS Omega 2025, 10, 17468−17475